European Polymer Journal 194 (2023) 112185

Contents lists available at ScienceDirect

European Polymer Journal

journal homepage: www.elsevier.com/locate/europolj

Disulfide vitrimeric materials based on cystamine and diepoxy eugenol as bio-based monomers

Adrià Roig [a], Marco Agizza [b], Àngels Serra [a,*], Silvia De la Flor [b,*]

[a] Universitat Rovira i Virgili, Department of Analytical and Organic Chemistry, C/ Marcel·lí Domingo 1, Edif. N4, 43007 Tarragona, Spain
[b] Universitat Rovira i Virgili, Department of Mechanical Engineering, Av. Països Catalans 26, 43007 Tarragona, Spain

ARTICLE INFO

Keywords:
Eugenol
Cystamine
Bio-based
Vitrimers
Disulfide
Internal catalysis

ABSTRACT

This study reports the synthesis and characterization of bio-based disulfide vitrimers obtained from diepoxy eugenol and cystamine through an epoxy-amine polycondensation process. TREN was added to the formulation in varying proportions to increase the crosslinking density. Although TREN reduced the number of disulfide groups in the vitrimers, it resulted in a maximum relaxation rate at a proportion of 25%. The vitrimers were characterized using FTIR, TGA, and thermomechanical analysis, and their T_g values, determined by DSC, ranged from 75 to 103 °C with increasing TREN proportion. The vitrimers rapidly relax with a relaxation time (τ) of 8.5 min at 170 °C. The addition of TREN decreased the relaxation times from 2.8 to 1.03 min by catalyzing the disulfide metathesis and achieving a balance between the proportion of disulfide bonds and the content of nucleophilic tertiary amines. Creep tests were performed at a wide range of temperatures to investigate the viscosity of the material below and above the T_gs. The topology freezing temperatures were calculated from the creep tests, and T_v values below T_g in all cases confirmed the catalytic effect of tertiary amines on the disulfide exchange reaction.

1. Introduction

Facing one of the most severe environmental problems today, which is the contamination of land and seas with plastic waste, the appearance of covalent adaptable networks (CANs) was a way to alleviate this problem [1]. Introducing exchangeable groups in the three-dimensional network of thermosets allows their reuse and recycling, significantly reducing the need for landfill disposal. The literature includes many chemically exchangeable groups; among them disulfide group is one of the most employed type of exchangeable group [2,3].

Although Tobolsky *et al.* noticed the possibility of stress relaxation in vulcanized rubbers in the 1960 s [4,5], disulfide vitrimers were developed from the pioneering work of Klumperman's group [6,7]. They demonstrated that the dynamic exchange reactions based on the disulfide bonds could be applied in the self-healing of epoxy-thiol thermosets, restoring their mechanical properties since disulfide exchange can be activated at a moderate temperature without the need for any catalysts. However, they concluded the limited applicability of the healing ability to low-T_g materials. After these studies, several authors included S-S bonds to the network structure to get reshapable and recyclable vitrimeric materials. Odriozola *et al.* reported the repairability, reprocessability, and recyclability of high T_g fiber-reinforced epoxy composites containing disulfide moieties [8]. Starting from commercially available DGEBA and 4-aminophenyl disulfide (4AFD), they obtain comparable mechanical performance to conventional materials.

Zhang *et al.* proved the effectiveness of tri-n-butyl phosphine in promoting the metathesis in disulfide epoxy networks. The reprocessed polymers showed self-healing ability and similar mechanical properties to the original materials [9]. Thus, due to the relatively weak S-S- bond, disulfides are the favorite dissociative links to improve self-healing properties of materials at mild temperatures [10].

Many studies focused on the disulfide exchange mechanism [11]. It was demonstrated that phosphines catalyzed disulfide metathesis. By quantum chemical studies, they determined that the rate-determining step is the nucleophilic attack of the phosphine to a sulfur, forming a thiolate and a R_3P^+ ^-SR cation. The reverse reaction is very fast and forms the catalyst and the disulfide bond [12]. In general, when nucleophiles are present in the material, there is an acceleration of the relaxation phenomena [13,14]. The homolytic cleavage of the disulfide bond followed by subsequent radical transfer of sulfur-based radicals

* Corresponding authors.
E-mail addresses: angels.serra@urv.cat (À. Serra), silvia.delaflor@urv.cat (S. De la Flor).

https://doi.org/10.1016/j.eurpolymj.2023.112185
Received 11 April 2023; Received in revised form 19 May 2023; Accepted 25 May 2023
Available online 30 May 2023

has also been confirmed [15]. The presence of carbon radicals, nucleophiles or free thiols affect the kinetics of disulfide exchange, and the mechanism can be dissociative or associative [16].

It is known that depending on the exchange mechanism, CANs can be divided into two main groups: dissociative or associative. In the first case, the mechanism goes through a dissociative pathway, meaning that a bond is broken and then formed in another place producing a sudden drop in the viscosity caused by the loss of the cross-linking density. In the second case, the bond exchange is produced in a concerted manner, without losing network integrity and with a gradual decrease of the viscosity with temperature [17]. This type of CANs is also named vitrimers because of their similar behavior with vitreous silica [1]. Nevertheless, there are also some exchange reactions that even being dissociative, the reforming of the bond is extremely fast, which from a physical point of view, a gradual decrease of the viscosity with temperature takes place following the Arrhenius law like vitrimers. These specific characteristics have been ascribed to vitrimer-like materials reported by Dichtel *et al.* [18].

Polysulfide materials could be self-healed and repaired through disulfide metathesis at room temperature when tributyl phosphine, pyridine, or triethylamine were used as catalysts [13]. However, using low-molecular-weight catalysts to accelerate the exchange reactions in vitrimeric materials presents some drawbacks since they can be exuded during the curing process, contaminating the environment. In addition, they can be easily eliminated at the high temperatures used in recycling and reshaping, reducing the catalytic effect. For this reason, it has been proposed the inclusion of nucleophiles, like tertiary amines, in the dynamic network structure [19]. In this field, Yamawake and co-workers reported the effects of internal tertiary amines on a disulfide cross-linked network [20]. They could see an enhancement on the creep resistance as well as in stress relaxation times when internal tertiary amines were incorporated in the polymer structure.

Using bio-based monomers in preparing recyclable thermosets is another excellent contribution to the sustainability of our planet. Most monomers are prepared from non-renewable fossil fuels that can be exhausted relatively quickly and contribute to global CO_2 emissions. The use of lignin [21], vanillin [22-24], eugenol [25], or phloroglucinol [26], among others, has been explored because the functional groups present in these products allow the synthesis of epoxy monomers. Recent reviews have been published highlighting the potential of these biomass-derived structures [22,27]. Some of these monomers were further reacted with 4-aminophenyl disulfide (4AFD), a commercially available disulfide source [22]. However, this aromatic diamine is not bio-based. As a bio-based disulfide containing amine, cystamine has been used. It is commercially available as a salt, but the corresponding amine can be obtained by extraction with a base. Torkelson *et al.* used this amine to cure epoxy novolac, obtaining a series of adaptative thermoset adhesives. The presence of the exchangeable S-S group allowed a significant enhancement in adhesive performance [28]. Recently, Guerre and co-workers also used cystamine as a crosslinker for the vanillin-based epoxy monomers. They use different proportions of cystamine and 4AFD to prepare different materials and could prove that the presence of the aliphatic hardener not only favors the curing kinetics but also the exchange process reducing the relaxation time ($\tau_{0.37}$) from 23 min to 22 s by changing the aromatic to the aliphatic amine [29].

The present article is devoted to preparing vitrimers from diepoxyeugenol, previously synthesized, and cystamine by a conventional epoxy-amine polycondensation. We have added to the formulation different proportions of tris(2-aminoethyl) amine (TREN) to increase the crosslinking density of the network structure and to increase the proportion of tertiary amines that can act as a catalyst in the disulfide exchange process, thus expecting to increase the relaxation process notably.

2. Materials and methods

2.1. Materials

Eugenol (EU), (±)-epichlorohydrin (ECH), benzyl trimethylammonium chloride (BTMA), acetic acid anhydride (AcAA), m-chloroperbenzoic acid (MCPBA), cystamine hydrochloride and tris(2-aminoethyl) amine (TREN) were purchased from Sigma-Aldrich.

Sodium hydroxide (granulated), sodium bicarbonate, potassium hydroxide, sodium chloride, magnesium sulphate and absolute ethanol (EtOH) were purchased from Scharlau. Dichloromethane (DCM), ethyl acetate and ethyl ether (Et_2O) were obtained from VWR Chemicals. All the reagents were used as received.

2.2. Preparation of acetyl eugenol (AcEU)

The synthesis of the diepoxy eugenol (DEPOEU) was made according to a reported procedure [30]. In a 250 mL three-neck round bottom flask equipped with a magnetic stirrer, thermometer, and reflux condenser, eugenol (16.4 g, 0.1 mol) and acetic anhydride (15.3 g, 0.15 mol) were reacted at 80 °C for 24 h. Once finished, ethyl ether was added, and the solution extracted twice with concentrated aqueous solutions of $NaHCO_3$ and NaCl. The organic layer was dried over anhydrous $MgSO_4$, and the solvent eliminated in a rotary evaporator. The pale orange viscous oil product (19.2 g, yield 93 %) was used in the following step without any further purification.

^{1}H NMR ($CDCl_3$; δ, ppm): 6.95 (d, 1H); 6.78 (m, 2H); 5.97 (m, 1H); 5.11 (m, 2H); 3.82 (s, 3H); 3.38 (d, 2H); 2.31 (s, 3H). (see Figure S1).

^{13}C NMR ($CDCl_3$; δ, ppm): 169.40, 150.95, 139.12, 138.09, 137.15, 122.62, 120.78, 116.26, 112.77, 55.90, 40.22, 20.82. (see Figure S2).

2.3. Synthesis of epoxy acetyl eugenol (EpAcEU)

The epoxidation of the allyl group of AcEU was done with MCPBA. In a 500 mL three-necked flask equipped with magnetic stirrer and ice bath, 17.6 g (0.085 mol) of AcEU were dissolved in 20 mL of DCM and then a solution of 30.4 g (0.13 mol) of MCPBA in 300 mL of DCM was added dropwise. The reaction was maintained at 0 °C for 24 h after complete disappearance of AcEU. The resulting DCM solution was extracted with a solution of $NaHSO_3$, then with concentrated aqueous solutions of $NaHCO_3$ and NaCl. The organic layer was dried over anhydrous $MgSO_4$, and the solvent eliminated in a rotary evaporator. EpAcEU was obtained as a viscous oil in a 95% of yield (18.0 g).

^{1}H NMR ($CDCl_3$; δ, ppm): 6.96 (d, 1H); 6.84 (m, 2H); 3.81 (s, 3H); 3.14 (m, 1H); 2.83 (d, 2H); 2.79 (t, 1H); 2.54 (dd, 1H); 2.29 (s, 3H) (see Figure S3).

^{13}C NMR ($CDCl_3$; δ, ppm): 169.27, 151.07, 138.58, 136.35, 122.78, 121.19, 113.29, 56.00, 52.45, 46.95, 38.76, 20.75 (see Figure S4).

2.4. Preparation of diepoxy eugenol (DEPOEU)

In a 250 mL round-bottomed flask equipped with reflux condenser and magnetic stirrer, 15.6 g of EpAcEU (0.07 mol) were dissolved in 45.3 g (0.49 mol) of epichlorohydrin. To this mixture, 5.6 g of NaOH (0.14 mol) in 30 mL of EtOH was added and the resulting solution was heated at 85 °C for 4 h and then left cooling to room temperature. Ethyl ether was added, and the salt formed removed by extraction with water. Then, the solution was dried over $MgSO_4$ anhydrous, filtered and ethyl ether removed in a rotary evaporator. The solid product obtained was purified by silica-gel column with a gradient hexane/ethyl acetate eluent: 4:1, 3:1, 2:1, and 1:1. The yield of the product after purification was 65 %. Melting point was 55.6 °C (by DSC).

^{1}H NMR ($CDCl_3$; δ, ppm): 6.87 (d, 1H); 6.77 (m, 2H); 4.22 (dd, 1H);

4.02 (dd, 1H); 3.86 (s, 3H); 3.37 (m, 1H); 3.12 (m, 1H); 2.87 (t, 1H); 2.79 (m, 3H); 2.73 (dd, 1H); 2.53 (dd, 1H) (see Figure S5).

^{13}C NMR ($CDCl_3$; δ, ppm): 149.60, 146.85, 131.07, 121.07, 114.34, 112.88, 70.44, 56.02, 52.65, 50.36, 46.9, 45.04, 38.40 (see Figure S6).

FTIR (ATR): 1600 cm^{-1} (Aromatics); 910 cm^{-1} (stretching glycidyl band); 835 cm^{-1} (stretching epoxide) (see Figure S7).

2.5. Preparation of the cystamine (Cys)

For the preparation of Cys, 8.0 g of cystamine dihydrochloride and 6.0 g of KOH were dissolved in 100 mL of distilled water. After stirring for 30 min at room temperature, the resulting mixture was extracted four times with DCM. The organic layers were combined, dried over anhydrous $MgSO_4$, and filtered. DCM was removed using a rotary evaporator obtaining 4.0 g of a yellowish viscous oil called cystamine (Cys). The pure cystamine must be used immediately after being obtained or it must be kept in a fridge.

^{1}H NMR ($CDCl_3$; δ, ppm): 2.95 (t, 4H); 2.70 (t, 4H); 1.28 (s, 4H) (see Figure S8).

^{13}C NMR ($CDCl_3$; δ, ppm): 42.55, 40.60 (see Figure S9).

2.6. General procedure for the preparation of vitrimeric samples

A series of the disulfide vitrimers were obtained according to the following procedure: DEPOEU was melted in a vial by heating at 65 °C. Then, the stoichiometric amount of mixtures in several proportions of Cys and TREN was added to the vial and the mixture was homogenized. The viscous mixture was poured into a Teflon mold with dimensions of 30 × 5 × 1.5 mm^3 and cured in an oven for 3 h at 100 °C, 1 h at 120 °C and 1 h at 150 °C to obtain transparent solid rectangular samples. The materials were coded as X% Cys, where X% means that X% of epoxides react with X% of NH groups coming from cystamine and (100-X) % of epoxides react with N–H groups coming from TREN. In all samples, the stoichiometric epoxy/NH ratio was maintained.

2.7. Characterization methods

^{1}H NMR and ^{13}C NMR spectra were registered in a Varian VNMR-S400 NMR spectrometer. $CDCl_3$ was used as a solvent. All chemical shifts are quoted on the δ scale in part per million (ppm) using residual protonated solvent as internal standard (^{1}H NMR: $CDCl_3$ = 7.26 ppm; ^{13}C NMR: $CDCl_3$ = 77.16 ppm).

DSC analyses were carried out on a Mettler DSC3 + instrument calibrated using indium (heat flow calibration) and zinc (temperature calibration) standards. Samples of approximately 8–10 mg were placed in aluminum pans with pierced lids and analyzed in an N_2 atmosphere with a glass flow of 50 cm^3 min^{-1}. Dynamic studies between 30 and 250 °C at a heating rate of 10 °C min^{-1} were performed to determine the melting points. For the determination of the T_gs of the final materials, dynamic experiments from 30 to 250 °C using a heating rate of 20 °C min^{-1} were performed.

A Jasco FT/IR-680 Plus spectrometer equipped with an attenuated total reflection accessory (ATR) (Golden Gate, Specac Ltd, Teknokroma) was used to record the FTIR spectra of the mixture before and after the curing procedure. Real-time spectra were recorded in the wavenumber range between 4000 and 600 cm^{-1} with a resolution of 4 cm^{-1} and averaged over 20 scans. The disappearance of the characteristic absorbance peaks of epoxy group at 915 and 830 cm^{-1} as well as the appearance of the peak corresponding to O—H at 3300 cm^{-1} were used to confirm the completion of the reaction.

The thermal stability of the materials was evaluated using a Mettler Toledo TGA 2 thermobalance. Cured samples weighing around 10 mg were degraded between 30 and 600 °C at a heating rate of 10 °C min^{-1} in N_2 atmosphere with a flow of 50 cm^3 min^{-1}.

The thermomechanical properties were studied using a DMTA Q800 (TA Instruments) equipped with a film tension clamp. Prismatic rectangular samples with dimensions around 30 × 5 × 1.5 mm^3 were analyzed from 0 °C to 200 °C at 1 Hz, with 0.1% strain at a heating rate of 2 °C min^{-1}. Tensile stress-relaxation tests were conducted in the same instrument using the film tension clamp on samples with the same dimensions as previously defined. The samples were firstly equilibrated at the relaxation temperature for 5 min, and a constant strain of 1% was applied, measuring the consequent stress level as a function of time. The materials were tested only once at one temperature. The relaxation-stress σ(t) was normalized by the initial stress σ_0, and the relaxation times (τ) were determined as the time necessary to relax 0.37σ_0, i.e., ($\sigma = 1/e\sigma_0$). With the relaxation times obtained at each temperature, the activation energy values (E_a), were calculated by using an Arrhenius-type equation:

$$\ln(\tau) = \frac{E_a}{RT} - \ln A$$

where τ is the time needed to attain a given stress-relaxation value (0.37σ_0), A is the pre-exponential factor, and R is the gas constant.

To determine the viscosity at each temperature needed for the representation of the Angell Fragility plot, a series of creep experiments were carried out on films at temperatures between 10 °C and 190 °C, increasing 10 °C in each scan. To perform the tests, the selected temperature was equilibrated for 3 min, and then a stress level of 0.1 MPa was applied for 30 min. The viscosity η (Pa·s) was then obtained from the strain–time graphs. First, the strain rate $\dot{\varepsilon}$ was determined from the slope of the graph, and the viscosity was calculated using the following equation:

$$\eta = \frac{\sigma}{\dot{\varepsilon}}$$

where σ is the stress applied during the test and $\dot{\varepsilon}$ the strain determined from the inverse of the slope of the strain–time curves. The viscosity was then plotted in front of the temperature, and the topology freezing temperature (T_v) was extrapolated by assuming that the viscosity at this temperature is 10^{12} Pa·s.

Finally, the Angell Fragility plot was represented by plotting the viscosity in front of T_v/T where the T_v is the one previously obtained.

3. Results and discussion

3.1. Synthesis of the diepoxy eugenol (DEPOEU)

DEPOEU was prepared *via* a three-step procedure, as reported in the literature [30]. Scheme 1 depicts the synthetic way adopted for synthesizing this product and the intermediates and the conditions of each step.

As we can see, there is an initial acetylation of the phenol group that protects it from undesired oxidation. Quin et al attempted the direct route of a first epoxidation of the allyl group, but the reaction mixture turned deep colored due to the possible conversion of phenol to quinone [30]. For this reason, they adopt this three-step synthetic process. Although we followed the same procedure, some experimental changes were introduced to improve the yield and purity of the intermediate and final compounds. All the synthetic intermediates and the final DEPOEU were characterized by NMR spectroscopy, and the corresponding spectra are collected in the SI.

Alternatively, the epoxidation of the allyl group of AcEU could be performed by the oxone method, which is more environmentally friendly than with MCPBA. In a previous work of our group, a triepoxy eugenol derivative was synthesized with good yields by this methodology [31]. However, the use of MCPBA to obtain EpAcEU resulted in a higher yield.

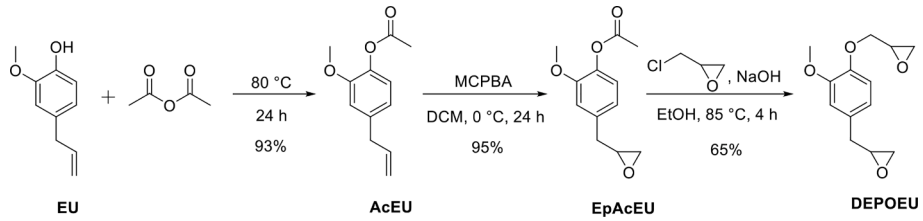

Scheme 1. Synthetic steps and reaction conditions used in the preparation of DEPOEU.

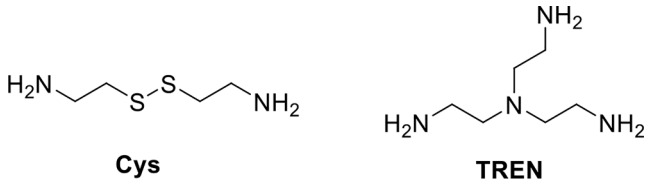

Scheme 2. Chemical structure of the amines used as curing agents.

3.2. Study of the curing procedure

The synthesized DEPOEU was cured with stoichiometric proportions of mixtures of Cys and TREN as amines of different functionality. Scheme 2 collects the chemical structure of both primary amines.

The composition of the formulations is detailed in Table 1.

Although adding TREN to the curing formulation reduces the proportion of exchangeable disulfide moieties, it also changes the crosslinking density and, consequently, some thermomechanical properties. In addition, the presence of the central nitrogen in the TREN structural unit can act as a catalyst. It has been established that the mechanical properties can be entirely restored after recycling, if 40 mol % of permanent crosslinks are included in the network structure [32]. Accordingly, we hypothesize that the addition of a certain proportion of TREN could not be detrimental to the relaxation process.

The curing process was investigated by DSC and the enthalpy released was around 95–100 kJ/eq, which is the typical for an epoxy-amine reaction [33,34]. The curing exotherm reach a maximum at 110 °C (Figure S10). Based on these results, the curing schedule selected was 3 h at 100 °C, 1 h at 120 °C, and 1 h at 150 °C.

The completion of the curing was confirmed by successive DSC scans to see if there is an increase in T_g, and by FTIR. FTIR spectra of the initial mixture of 100%Cys and the corresponding final material is shown in Fig. 1, where we can see the disappearance of the epoxy bands at 915 and 835 cm^{-1} and the broad absorption around 3400 cm^{-1} due to the formation of the OH groups.

3.3. Thermal characterization of the materials

Once cured, the materials obtained were first characterized by DSC. As expected, increasing the proportion of TREN to the formulation led to an increase in the T_g values. Table 2 collects the T_gs of all the materials prepared. The DSC traces are shown in Figure S11.

The thermal stability of the vitrimeric materials was determined by thermogravimetry. Fig. 2 shows the TGA curves and their derivatives for the materials prepared, and Table 2 presents the most significant data extracted.

Due to the weakness of S-S bond, the higher its proportion, the faster the degradation at lower temperatures. In all the samples, there is a first degradation step corresponding to the breakage of the S-S bond, while in the second step, there is not much difference among the materials since all the bonds break simultaneously.

The thermogravimetric study confirms that safe relaxation processes can proceed at temperatures below 200 °C.

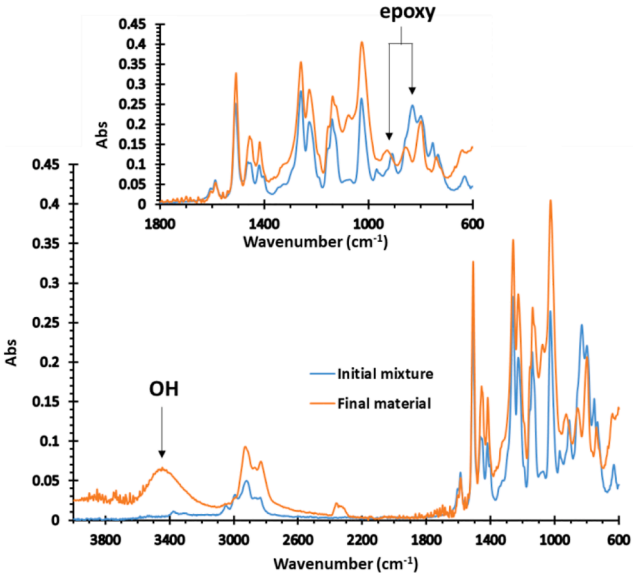

Fig. 1. FTIR-ATR spectra of the 100%Cys initial mixture (blue) and final material (orange). (For interpretation of the references to colour in this figure legend, the reader is referred to the web version of this article.)

Table 1
Composition of all the vitrimeric materials prepared.

Sample	DEPOEU		Cys		TREN	
	wt (%)	mmol	wt (%)	mmol	wt (%)	mmol
100%Cys	76.0	4.23	24.0	2.12	–	–
85%Cys	76.6	4.23	21.0	1.80	2.4	0.21
75%Cys	77.3	4.23	18.7	1.59	4.0	0.35
65%Cys	78.0	4.23	16.4	1.38	5.6	0.49
50%CyS	79.1	4.23	12.7	1.05	8.2	0.71

Table 2
Glass transition temperature by DSC, temperature of initial degradation, temperatures of the maximum degradation rate and residue at 600 °C.

Sample	T_g (°C)	$T_{1\%}$[a] (°C)	$T_{2\%}$[b] (°C)	T_{max}[c] (°C)	Char Yield (%)
100%Cys	74.9	210.1	244.1	273.8/328.0	23.2
85%Cys	80.9	213.8	250.1	272.9/335.2	25.3
75%Cys	84.9	225.0	263.8	272.5/335.5	25.5
65%Cys	90.2	235.4	268.9	277.0/341.8	25.6
50%Cys	102.9	250.6	270.6	273.4/338.2	25.7

[a]Temperature of 1% weight loss.
[b]Temperature of 2% weight loss.
[c]Temperature of the two maximum rates of degradation.
[d]Char residue at 600 °C.

3.4. Thermomechanical characterization of the materials

The thermomechanical characteristics of the materials were determined by DMTA. Fig. 3 shows the evolution of the storage moduli and tan δ curves with the temperature for all the materials prepared, and

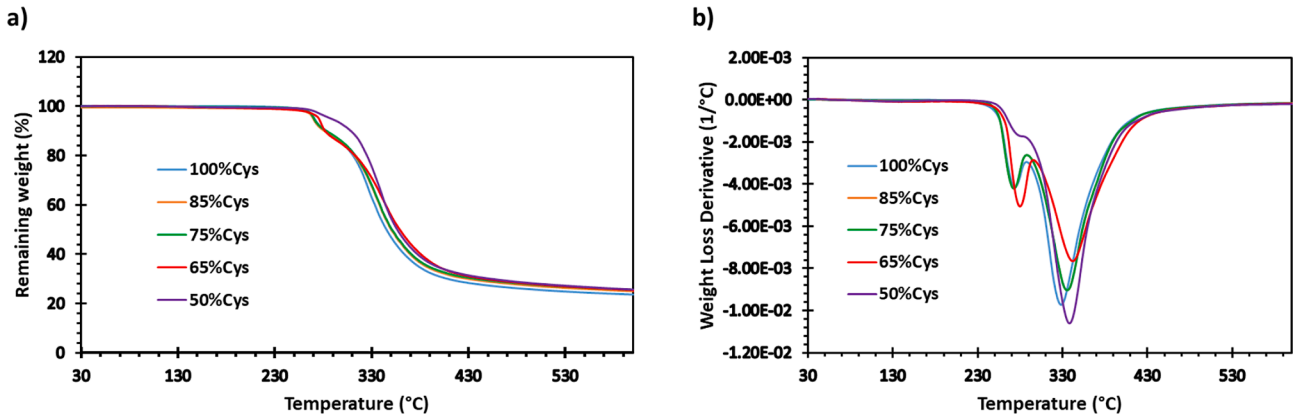

Fig. 2. (a) Thermogravimetric analysis (TGA) curves and (b) DTG curves of the vitrimeric materials prepared.

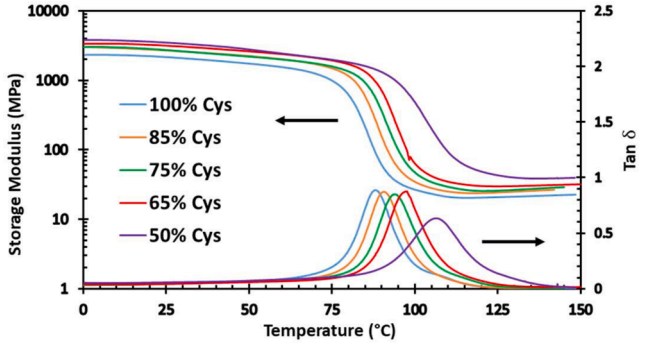

Fig. 3. Evolution of storage modulus and tan δ with the temperature for all the materials.

Table 3
Main thermomechanical parameters obtained for the different materials.

Sample	E'_{glassy} [a] (MPa)	$E'_{rubbery}$ [b] (MPa)	$T_{tan\ \delta}$ [c] (°C)	FWHM [d] (°C)
100%Cys	1890	21.9	88.2	12.5
85%Cys	2330	26.4	90.7	12.9
75%Cys	2420	28.8	93.9	13.7
65%Cys	2550	31.7	97.6	18.8
50%Cys	2670	39.6	106.4	24.6

[a] Storage Modulus in the glassy state at Tg −50 °C.
[b] Storage Modulus in the rubbery state at Tg + 50 °C.
[c] Temperature of the maximum of the of tan δ peak.
[d] Full width at the half height of tan δpeak.

Table 3 collects the main parameter extracted from these studies.

As it can be seen, all materials exhibit high T_g values (taken from the maximum of the $T_{tan\delta}$peak) ranging from 88 °C for 100%Cys to 106 °C for 50%Cys. As expected, the higher the proportion of cystamine in the material, the lower the $T_{tan\delta}$ since it has a longer chain and fewer possible cross-linking points, providing more flexibility to the networks. Moreover, when the proportion of Cys is decreased, the E'_{glassy} increases due to the higher proportion of TREN in the samples making the materials more rigid. The same trend can be observed in the $E'_{rubbery}$ since the higher functionality of TREN increases the storage moduli in the rubbery state, which is directly connected to the crosslinking density of the material. Looking at the shape of the tanδ curves and the low values of FWHM, it can be deduced that all the materials present homogeneous and fast transitions. The material with 50%Cys, with a slightly broader (higher FWHM) and less intensity (lower height of tanδ peak) indicates its more crosslinked structure.

3.5. Study of the vitrimeric behavior of the materials

Cystamine contains disulfide bonds in its structure, so it is expected to provide final materials with vitrimeric properties through the disulfide metathesis reaction at high temperatures. To investigate the time and temperature-dependent relaxation, stress relaxation tests at different temperatures for all materials were performed in the DMTA. The results for each material are shown in Figures S12-S16, and the data is presented in Table 4. As a mode of comparison, stress relaxation curves for all materials at 170 °C are represented in Fig. 4.

As shown in Fig. 4a, intriguing results were obtained regarding the relaxation times of the samples. The main data extracted from these tests are presented in Table 4. 100%Cys material presents the highest proportion of disulfide bonds in its structure, so it is likely the one that should relax the initial stress in a faster way. Indeed, it only needs 2.8 min to achieve the $0.37\sigma_0$. However, it was observed that when the proportion of Cys is slightly reduced, faster relaxation times are achieved, being 2.75 min for 85%Cys and 1.03 min for 75%Cys. This decrease in the relaxation times can be ascribed to the catalytic effect of the tertiary amines on the disulfide metathesis exchange. When the amount of TREN in the samples increases, the concentration of tertiary

Table 4
Relaxation time, activation energy and adjusting parameters from Arrhenius plot.

Material	$\tau_{0.37}$ [a] (min)	E_a (kJmol^{-1})	ln A (min)	r^2	$T_{v\ (\eta)}$ [b] (°C)	$T_{v\ (Angell)}$ [c] (°C)	n [d]
100%Cys	2.80	85.7	22.26	0.991	66.7	77.0	7.12
85%Cys	2.75	81.5	21.19	0.995	67.1	60.1	4.82
75%Cys	1.03	95.5	25.34	0.993	34.2	26.8	3.04
65%Cys	6.30	41.1	9.61	0.971	57.5	57.6	3.09
50%Cys	8.44	42.9	10.49	0.983	54.4	59.4	1.77

[a] Time reach a value of $\sigma/\sigma_0 = 0.37$ at 170 °C.
[b] Topology freezing temperature calculated by extrapolation of the η-T curves.
[c] Topology freezing temperature calculated by extrapolation from the adjusting of the Angell fragility plot.
[d] Fragility index ($n_{silica} = 16.5$).

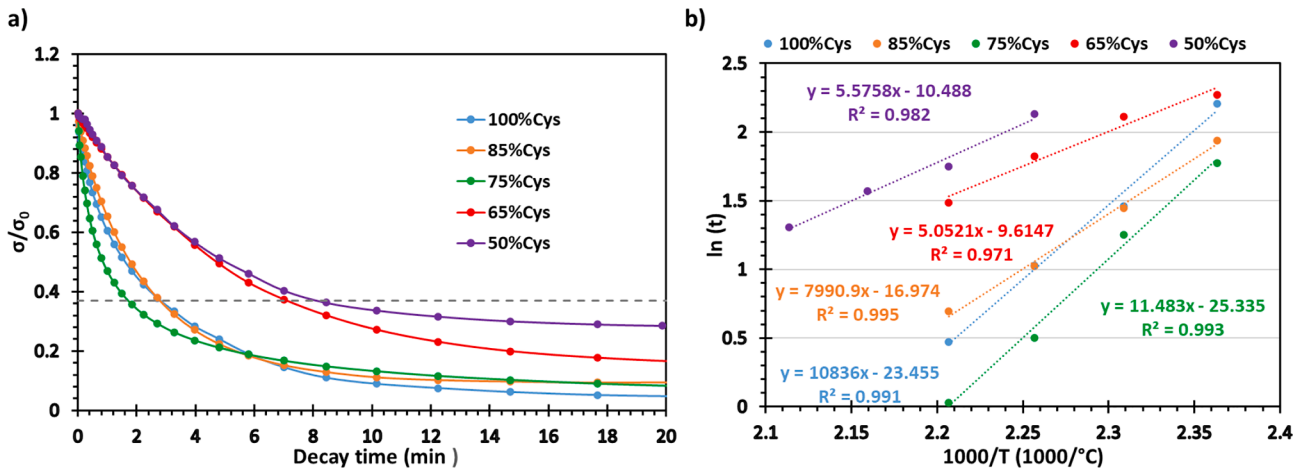

Fig. 4. a) Normalized stress relaxation curves as a function of time for all the materials prepared at 170 °C. b) Arrhenius plots for the relaxation times with the inverse of temperature for all samples.

amines in the materials is higher because TREN contains four tertiary amines in its structure while cystamine only has two. It is worth highlighting that a maximum is reached in the 75%Cys material where the concentration of disulfide bonds is still high to get a fast relaxation but, at the same time, the content of tertiary amines in the network is high enough to increase the catalytic effect on the disulfide metathesis. Nevertheless, when the proportion of Cys is lowered, a detrimental effect in the relaxation times can be noticed since the amount of disulfide bonds is relatively low, even containing a higher proportion of internal tertiary amines. Moreover, one can notice that even though the 75%Cys material can relax the 63% of the initial stress faster, it cannot achieve complete relaxation since the percentage of permanent crosslinks is relatively high. In this case, the higher proportion of cystamine in the material, the fewer permanent crosslinks in the network and, therefore, the more able to fully relax the initial stress.

A linear relationship between temperature and viscosity is established when the exchange reactions occur in the materials network. For this reason, the stress relaxation times at different temperatures, when the materials relax the 63% of the initial stress, were obtained from Figures S12-S16. They all follow an Arrhenius-type dependence, like vitrimers, which allows calculating the activation energy (E_a) and the ln A. These values are also presented in Table 4 and the plot is represented in Fig. 4b.

As seen in Table 4, the behavior of all the materials fit the Arrhenius equation with different E_a values depending on the network composition. 75%Cys material has the highest activation energy showing a high dependence between the relaxation times and the temperature, meaning that a slight temperature change significantly affects the relaxation time, which is in accordance with the high content in tertiary amines and disulfide bonds.

The effect of the temperature on the viscosity was also studied through creep tests at different temperatures in DMTA for all the materials. Creep tests from temperatures far below the T_g of the materials to far above were performed on all the materials. The viscosity (inverse of the slope of the ε·t curves) was plotted versus the temperature for all cases. (Figures S17-S21).

As seen in these figures, all materials show the same trend where, well below the onset of the glass transition, the viscosity of the vitrimers follows a somehow linear behavior with temperature. During the transition of the T_g, the bond exchange can be described via William-Landel-Ferry (WLF) behavior as the network rearrangement kinetics is diffusion-controlled and segmental motions dominate network rearrangement [35,36]. After that, with a further temperature increase, the exchange kinetics change to an exchange reaction-controlled regime. Consequently, the disulfide metathesis again follows a linear Arrhenius law in all cases.. The topology freezing temperature (T_v) of all materials can be calculated from these plots since, by a physical definition, is the temperature at which the material reaches a viscosity of 10^{12} Pa·s. All T_vs were calculated by extrapolation from the graphs and are depicted in Table 4. As shown in the table, all the materials presented T_v values below T_gs which is consequent with the viscosity behavior obtained for all these vitrimers [37,38]. On the other hand, the T_v can also be ascribed to the temperature below which the exchange mechanisms are almost negligible [1]. 75%Cys material has the lowest topology freezing temperature, which fits with the evidence that a compromise between the concentration of disulfide bonds in the network and the proportion of tertiary amines enhances the exchange reaction. In addition, it should be highlighted that when the content of internal tertiary amines is increased in the network (50%Cys and 65%Cys) the T_v is lower than in the materials with almost no TREN content (100%Cys and 85%Cys), demonstrating a high dependence of the T_v with the internal load of catalysts.

From the results obtained in the creep tests, the Angell fragility plots can also be represented (Fig. 5). As it is known, at higher temperatures, the chemical exchange reactions control the viscosity of the vitrimers, thus producing its gradual decrease as the temperature increase and following an Arrhenius law, similar to inorganic silica materials. On the other hand, dissociative CANs and thermoplastics evolve abruptly from a solid to a liquid state with a sudden viscosity drop when the temperature increases. In our case, all the materials experienced a gradual decrease in viscosity, meaning that they present vitrimeric-like

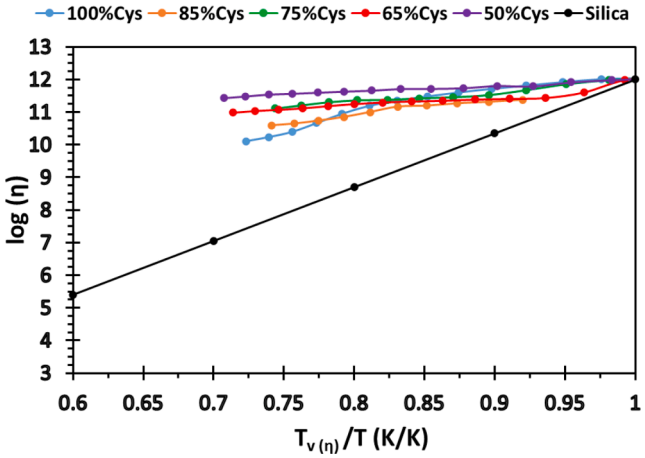

Fig. 5. Angell fragility plots for all the materials prepared.

properties [39]. It has been reported that the S-S exchange mechanism can also be performed by the attack of a thiolate anion which can be generated in the presence of a tertiary amine and the consequent nucleophilic attack of this thiolate on another disulfide bond further generating another thiolate [20]. This mechanism may provide an associative pathway to exchange process which is in accordance with the vitrimer-like behavior observed in our materials in the Angell Fragility plot. These results indicate that even the mechanism of disulfide metathesis is purely dissociative, when tertiary amines are covalently attached to the network, the mechanism may follow an associative mechanism. This can explain the gradual decrease in the viscosity with temperature in our materials, thus behaving like vitrimer-like polymers. It is important to highlight the novelty of present studies, which were performed on bio-based materials that were cured with aliphatic amines containing aliphatic disulfide bonds. Even so, these results are in accordance with previous studies in aromatic disulfide materials performed by Rekondo and co-workers, who reported a similar trend in their materials [14].

Finally, the T_vs from the linear equations deduced from the Angell plot can also be calculated by assuming that the materials reach a viscosity of 10^{12} Pa·s and therefore, $\log(\eta_{(Tv)}) = 12$. The values extracted from these extrapolations are shown in Table 4. Logically, all T_vs were very similar to those ones obtained from creep tests.

4. Conclusions

A bio-based diepoxy eugenol (DEPOEU) derivative was synthesized via a three-step method and crosslinked with varying proportions of cystamine and TREN via an epoxy-amine condensation reaction. FTIR analysis confirmed successful curing and completion of the reaction. The resulting materials exhibited high thermal stability ($T_{1\%} > 210$ °C) and T_gs ranging from 74.9 °C (for the 100%Cys) to 102.9 °C (for the 50% Cys).

The exchange reaction was facilitated by the disulfide bonds of cystamine, with the addition of TREN enhancing the exchange rate. All materials could rapidly relax the 63% of the initial stress in less than 8.5 min. Interestingly, even the 100%Cys material that relaxes more is not the one with lower relaxation rates. The addition of TREN and, therefore, the increase of tertiary amines in the crosslinked structure catalyzes the exchange reaction. The 75%Cys material demonstrated the optimal balance of S-S bonds and tertiary amines, exhibiting the fastest relaxation rate of 63% in just 1.03 min.

The topology freezing temperature (T_v) was calculated via creep tests, being below T_g in all cases. The 75%Cys material exhibited the lowest T_v, evidencing the compromise mentioned above. The Angell fragility plot also revealed the vitrimeric behavior of all the materials. Overall, these results suggest that the DEPOEU-based materials have great potential as vitrimers for use in a great variety of applications, such as coatings, adhesives, and composite materials.

CRediT authorship contribution statement

Adrià Roig: Investigation, Writing – original draft. **Marco Agizza:** Investigation. **Àngels Serra:** Conceptualization, Funding acquisition, Writing – review & editing. **Silvia De la Flor:** Conceptualization, Methodology, Writing – review & editing.

Declaration of Competing Interest

The authors declare that they have no known competing financial interests or personal relationships that could have appeared to influence the work reported in this paper.

Data availability

Data will be made available on request.

Acknowledgments

This work is part of the R&D project PID2020-115102RB-C21 funded by MCNI/AEI/10.13039/501100011033 and European Union NextGenerationEU"/PRTR. We acknowledge these grants and to the Generalitat de Catalunya (2021-SGR-00154).

Appendix A. Supplementary material

Supplementary data to this article can be found online at https://doi.org/10.1016/j.eurpolymj.2023.112185.

References

[1] D. Montarnal, M. Capelot, F. Tournilhac, L. Leibler, Silica-like malleable materials from permanent organic networks, Science 334 (2011) 965–968, https://doi.org/10.1126/science.1212648.
[2] S. Samanta, S. Kim, T. Saito, A.P. Sokolov, Polymers with dynamic bonds: adaptive functional materials for a sustainable future, J. Phys. Chem. B 125 (2021) 9389–9401, https://doi.org/10.1021/acs.jpcb.1c03511.
[3] W. Zhang, Y. Jing, Eds. Dynamic Covalent Chemistry. Principles, Reactions, and Applications. Ed. Wiley, 2018, Pondicherry, India.
[4] A.V. Tobolsky, W.J. MacKnight, M. Takahashi, Relaxation of disulfide and tetrasulfide polymers, Phys. Chem. 68 (1964) 787–790, https://doi.org/10.1021/j100786a013.
[5] Y. Takahashi, A.V. Tobolsky, Chemorheological study on natural rubber vulcanizates, Polym. J. 2 (1971) 457–467, https://doi.org/10.1295/polymj.2.457.
[6] J. Canadell, H. Goossens, B. Klumperman, Self-healing materials based on disulfide links, Macromolecules 44 (2011) 2536–2541, https://doi.org/10.1021/ma2001492.
[7] M. Pepels, I. Filot, B. Klumperman, H. Goossens, Self-healing systems based on disulfide-thiol exchange reactions, Polym. Chem. 4 (2013) 4955–4965, https://doi.org/10.1039/C3PY00087G.
[8] A. Ruiz de Luzuriaga, R. Martin, N. Markaide, A. Rekondo, G. Cabañero, J. Rodríguez, I. Odriozola, Epoxy resin with exchangeable disulfide crosslinks to obtain reprocessable, repairable and recyclable fiber-reinforced thermoset composites, Mater. Horiz. 3 (2016) 241–247, https://doi.org/10.1039/C6MH00029K.
[9] Z.Q. Lei, H.P. Xiang, Y.J. Yuan, M.Z. Rong, M.Q. Zhang, Room-temperature self-healable and remoldable cross-linked polymer based on the dynamic exchange of disulfide bonds Chem, Mater. 26 (2014) 2038–2046, https://doi.org/10.1021/cm4040616.
[10] M. Podgórski, B.D. Fairbanks, B.E. Kirkpatrick, M. McBride, A. Martinez, A. Dobson, N.J. Bongiardina, C.N. Bowman, Toward stimuli-responsive dynamic thermosets through continuous development and improvements in covalent adaptable networks (CANs), Adv. Mater. 32 (2020) 1906876, https://doi.org/10.1002/adma.201906876.
[11] N.J. Bongiardina, S.M. Soars, M. Podgórski, C.N. Bowman, Radical-disulfide exchange in thiol-ene-disulfidation polymerizations, Polym. Chem. 13 (2022) 3991–4003, https://doi.org/10.1039/D2PY00172A.
[12] R. Caraballo, M. Rahm, P. Vongvilai, T. Brinck, O. Ramström, Phosphine-catalyzed disulfide metathesis, Chem. Commun. 46 (2008) 6603–6605, https://doi.org/10.1039/B815710C.
[13] S.J. Tonkin, C.T. Gibson, J.A. Campbell, D.A. Lewis, A. Karton, T. Hasell, J. M. Chalker, Chemically induced repair, adhesion, and recycling of polymers made by inverse vulcanization, Chem. Sci. 11 (2020) 5537–5546, https://doi.org/10.1039/D0SC00855A.
[14] A. Ruiz de Luzuriaga, G. Solera, I. Azcarate-Ascasua, V. Boucher, H.J. Grande, A. Rekondo, Chemical control of the aromatic disulfide exchange kinetics for tailor-made epoxy vitrimers, Polymer 239 (2022), 124457, https://doi.org/10.1016/j.polymer.2021.124457.
[15] S. Nevejans, N. Ballard, J.I. Miranda, B. Reck, J.M. Asua, The underlying mechanisms for self-healing of poly(disulfide)s, Phys. Chem. Chem. Phys. 18 (2016) 27577–27583, https://doi.org/10.1039/C6CP04028D.
[16] A.G. Orrillo, R.L.E. Furlan, Sulfur in Dynamic covalent chemistry, Angew. Chem. Int. Ed. 61 (2022) e202201168.
[17] F. Van Lijsebetten, J.O. Holloway, J.M. Winne, F.E. Du Prez, Internal catalysis for dynamic covalent chemistry applications and polymer science, Chem. Soc. Rev. 49 (2020) 8425–8438, https://doi.org/10.1039/D0CS00452A.
[18] B.R. Elling, W.R. Dichtel, Reprocessable cross-linked polymer networks: are associative exchange mechanisms desirable? ACS Cent. Sci. 6 (2020) 1488–1496, https://doi.org/10.1021/acscentsci.0c00567.
[19] F.I. Altuna, C.E. Hoppe, R.J.J. Williams, Epoxy vitrimers with a covalently bonded tertiary amine as catalyst for the transesterification reaction, Eur. Polym. J. 113 (2019) 297–304, https://doi.org/10.1016/j.eurpolymj.2019.01.045.
[20] K. Yamawake, M. Hayashi, The role of tertiary amines as internal catalysts for disulfide exchange in covalent adaptable networks, Polym. Chem. 14 (2023) 680–686, https://doi.org/10.1039/D2PY01406H.
[21] A. Moreno, M. Morsali, M.H. Sipponen, Catalyst-free synthesis of lignin vitrimers with tunable mechanical properties: circular polymers and recoverable adhesives, ACS Appl. Mater. Interfaces 13 (2021) 57952–57961, https://doi.org/10.1021/acsami.1c17412.

[22] M.A. Rashid, N. Hasan, A.R. Dayan, M.S.I. Jamal, M.K. Patoary, A critical review of sustainable vanillin-modified vitrimers: synthesis, challenge and prospects, Reactions 4 (2023) 66–91, https://doi.org/10.3390/reactions4010003.
[23] A. Roig, A. Petrauskaitė, X. Ramis, S. De la Flor, À. Serra, Synthesis and characterization of new bio-based poly(acylhydrazone) vanillin vitrimers, Polym. Chem. 13 (2022) 1510–1519, https://doi.org/10.1039/D1PY01694F.
[24] A. Roig, P. Hidalgo, X. Ramis, S. De la Flor, À. Serra, Vitrimeric epoxy-amine polyimine networks based on a renewable vanillin derivative, ACS Appl. Polym. Mater. 4 (2022) 9341–9350, https://doi.org/10.1021/acsapm.2c01604.
[25] T. Liu, C. Hao, L. Wang, Y. Li, W. Liu, J. Xin, J. Zhang, Eugenol-derived biobased epoxy: shape memory, repairing, and recyclability, Macromolecules 50 (2017) 8588–8597, https://doi.org/10.1021/acs.macromol.7b01889.
[26] A. Genua, S. Montes, I. Azcune, A. Rekondo, S. Malburet, B. Daydé-Cazals, A. Graillot, Build-to-specification vanillin and phloroglucinol derived biobased epoxy-amine vitrimers, Polymers 12 (2020) 2645, https://doi.org/10.3390/polym12112645.
[27] M.A. Lucherelli, A. Duval, L. Avérous, Biobased vitrimers: Towards sustainable and adaptable performing polymer materials, Prog. Polym. Sci. 127 (2022), 101515, https://doi.org/10.1016/j.progpolymsci.2022.101515.
[28] L. Li, X. Chen, J.M. Torkelson, Covalent adaptive networks for enhanced adhesion: exploiting disulfide dynamic chemistry and annealing during application, ACS Appl. Polym. Mater. 2 (2020) 4658–4665, https://doi.org/10.1021/acsapm.0c00720.
[29] S. Guggari, F. Magliozzi, S. Malburet, A. Graillot, M. Destarac, M. Guerre, Vanillin-based epoxy vitrimers: looking and the cystamine hardener form a different perspective, ACS Sustainable Chem. Eng. 11 (2023) 6021–6031, https://doi.org/10.1021/acssuschemeng.3c00379.
[30] J. Qin, H. Liu, P. Zhang, M. Wolcott, J. Zhang, Use of eugenol and rosin as feedstocks for biobased epoxy resins and study of curing performance properties, Polym. Int. 63 (2014) 760–765, https://doi.org/10.1002/pi.4588.
[31] D. Guzmán, X. Ramis, X. Fernández-Francos, S. De la Flor, A. Serra, Preparation of new biobased coating from a triglycidyl eugenol derivative through thiol-epoxy click reaction, Prog. Org. Coat. 114 (2018) 259–267, https://doi.org/10.1016/j.porgcoat.2017.10.025.
[32] L. Li, X. Chen, K. Jin, J.M. Torkelson, Vitrimers designed both to strongly suppress creep and to recover original cross-link density after reprocessing: quantitative theory and experiments, Macromolecules 51 (2018) 5537–5546, https://doi.org/10.1021/acs.macromol.8b00922.
[33] K.J. Ivin, Polymer Handbook, Wiley, New York, 1975.
[34] A. Roig, X. Ramis, S. De la Flor, À. Serra, Dual-cured thermosets from glycidyl methacrylate obtained by epoxy-amine reaction and methacrylate homopolymerization, React. Funct. Polym. 159 (2021), 104822, https://doi.org/10.1016/j.reactfunctpolym.2021.104822.
[35] M.T. Shaw, W.J. MacKnight, Introduction to polymer viscoelasticity; wiley: hoboken, NJ, USA, 2005.
[36] L.H. Sperling, Introduction to physical polymer science, wiley: Hoboken, NJ, USA, 2005.
[37] B. Krishnakumar, R.V.S.P. Sanka, W.H. Binder, V. Parthasarthy, S. Rana, N. Karak, Vitrimers: associative dynamic covalent adaptive networks in thermoset polymers, Chem. Eng. J. 385 (2020), 123820, https://doi.org/10.1016/j.cej.2019.123820.
[38] Y. Nishimura, J. Chung, H. Muradyan, Z. Guan, Silyl ether as a robust and thermally stable dynamic covalent motif for malleable polymer design, J. Am. Chem. Soc. 139 (2017) 14881–14884, https://doi.org/10.1021/jacs.7b08826.
[39] W. Denissen, J.M. Winne, F.E. Du Prez, Vitrimers: permanent organic networks with glass-like fluidity, Chem. Sci. 7 (2016) 30–38, https://doi.org/10.1039/C5SC02223A.